

Comparative Study of Rotational and Longitudinal Turning: Energy Efficiency and Surface Roughness in Machining Normalized Medium-Carbon Steel

István Sztankovics

Associate Professor

University of Miskolc

Faculty of Mechanical Engineering

and Informatics

Institute of Manufacturing Science

Hungary

Dragan Rodić

Associate Professor

University of Novi Sad

Faculty of Technical Sciences

Department for Production Engineering

Serbia

This study compares rotational and longitudinal turning during the machining of normalized medium-carbon steel. The aim is to evaluate differences in energy efficiency and surface quality. Three tools were tested: two rotational turning tools with 30° and 45° inclination angles and a conventional longitudinal turning tool. Thirty-six cutting experiments were performed while varying depth of cut, feed, and cutting speed. Cutting forces were measured in three directions and used to calculate specific cutting forces and total mechanical work. Surface roughness was evaluated using arithmetical mean roughness and maximum peak-to-valley height parameters. The results show that rotational turning, particularly with a 30° inclination, reduces specific cutting forces and enables lower energy consumption at comparable productivity. It also provides better surface finish at medium and high feeds. Longitudinal turning generated acceptable energy levels but produced significantly rougher surfaces. The findings highlight the role of tool inclination in improving energy-surface-quality interactions.

Keywords: Energy efficiency, Machining, Medium-carbon steel, Rotational turning, Specific cutting force, Surface roughness.

1. INTRODUCTION

In the field of manufacturing engineering, the demand for energy-efficient and high-quality machining processes has intensified significantly in recent years [1,2]. This growing importance is largely driven by economic and environmental concerns, paired with the increasing need for precision and consistency in the production of mechanical components. Among the various machining operations, turning remains one of the most fundamental and widely applied processes for shaping rotationally symmetric parts such as shafts, bushings, and bearing components [3,4]. Despite its apparent developed state, the turning process continues to be an active area of research due to its critical role in productivity, surface integrity, and overall process sustainability [5,6].

Traditionally, turning operations are performed using a longitudinal feed strategy, where the cutting tool moves parallel to the axis of the rotating workpiece [7]. This method has been the pillar of cylindrical machining and is well-documented in both industrial practice and scientific literature. However, recent advancements in tooling concepts and kinematic alternatives have led to the development of non-traditional turning strategies [8,9], among which rotational turning (also referred to as tangential turning with circular feed movement) has

gained increasing attention [10-12]. In rotational turning, the cutting edge is oriented at an angle to the workpiece axis and a circular secondary feeding movement is applied [13,14], introducing a fundamentally different engagement between the cutting edge and the material.

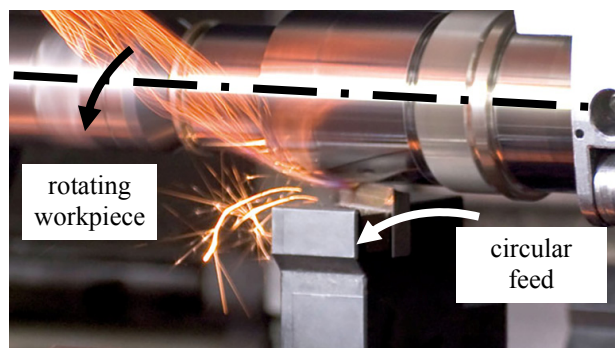


Figure 1. Rotational turning [14]

This alternative approach offers unique advantages in chip formation, force distribution, and tool wear behaviour, and it has potential for specific applications where the application of conventional methods are limited. The motivation for exploring rotational turning lies in its ability to address challenges that are difficult to overcome with longitudinal turning. These include tool vibration, heat concentration, and unfavourable force component distributions, which can lead to early tool wear, poor surface finish, and excessive energy consumption. The introduction of an inclination angle in rotational turning modifies the chip load distribution and contact geometry, which can influence both the cutting forces and the

Received: September 2025, Accepted: December 2025

Correspondence to: Dr. István Sztankovics

Institute of Manufacturing Science, University of Miskolc, Miskolc-Egyetemváros, H-3515, Hungary

E-mail: istvan.sztankovics@uni-miskolc.hu

doi: 10.5937/fme2601039S

© Faculty of Mechanical Engineering, Belgrade. All rights reserved

resulting surface topography [15,16]. Consequently, this modified kinematics can enable higher productivity under certain conditions, especially when combined with optimized cutting parameters.

Despite the promising nature of rotational turning, there remains a lack of comprehensive studies that directly compare its performance with conventional longitudinal turning under controlled and repeatable experimental conditions. This is particularly true for studies that jointly evaluate energy efficiency and surface quality, which are critical performance indicators in modern manufacturing [17,18]. Most existing literature tends to focus on either force analysis or surface integrity in isolation, often without considering the broader context of process sustainability and machinability. Moreover, the influence of tool inclination angle – a key parameter in rotational turning – on energy consumption and surface roughness is still not fully understood, especially when machining common engineering materials such as medium-carbon steels. Medium-carbon steels, including normalized C45 steel, are widely used in the manufacturing of automotive, structural, and machinery components due to their good balance of strength, machinability, and cost-effectiveness [19,20]. Although not regarded as a high-performance alloy, C45 represents a class of workpiece materials that is highly relevant in industry and thus serves as a meaningful subject for comparative machining studies [21-23]. The machining of normalized C45 presents moderate cutting resistance, making it suitable for evaluating process-induced differences in energy demand and surface finish across various tool geometries and feed strategies.

To quantify energy efficiency, cutting forces should be measured using a high-precision dynamometer [24,25]. From the force components, the mechanical work done during cutting could be calculated, which serves as a direct indicator of energy consumption in the material removal process. In addition, the specific cutting force values could be calculated to normalize the data and enable meaningful comparisons across different setups. These parameters are particularly useful in evaluating the effectiveness of each turning strategy in terms of material removal efficiency [26-28]. Beyond evaluating machining forces and energy consumption, cutting-force measurements also provide essential input for analysing the dynamic behaviour of turning tools. Studies have demonstrated that measured cutting forces can be integrated into analytical or numerical models to estimate tool displacement and vibration response during turning operations [29,30]. Cutting-force data are equally valuable in stability investigations, where they support the development and validation models used to study chatter behaviour, forced vibration, and the performance of advanced tool-holder structures [31,32]. These applications highlight that high-quality force measurements are not only important for analysing cutting mechanics but also play a central role in understanding and improving the dynamic stability and vibration resistance of turning processes.

In parallel with force and energy measurements, surface roughness is often characterized using two widely accepted parameters: arithmetical mean roughness and maximum height of the roughness profile. These

values provide complementary insights into the quality of the machined surfaces. The analysis of these parameters assists the identification of surface finish trends associated with different tool geometries and cutting conditions [33-35]. The wider literature also shows that surface roughness evaluation plays a central role in many machining studies, even when the work materials or machining strategies differ from the present work. For example, investigations have shown that both cutting tool geometry and process parameters strongly influence surface roughness and dimensional accuracy, with high cutting speeds and low feed rates leading to improved surface quality [36,37]. Other studies have focused on the prediction of surface roughness using data-driven approaches, where image processing combined with machine learning techniques has achieved high correlation levels when estimating roughness parameter values [38,39]. Furthermore, studies have confirmed that surface roughness is strongly dependent on feed rate, which often emerges as the dominant parameter influencing machinability, while excessive depth of cut may lead to undesirable increases in cutting force and degradation in surface finish [40-42]. These examples underline the broad applicability of roughness-based evaluation across machining research and support the need for detailed surface characterization in comparative studies such as this.

The present study addresses these gaps by conducting a systematic comparative investigation of rotational and longitudinal turning, focusing on the energy efficiency and surface roughness characteristics achieved when machining normalized medium-carbon steel. Three tool configurations are used: a standard longitudinal turning tool and two rotational turning tools with inclination angles of 30° and 45°, respectively. The experiments cover a range of cutting parameters, including different feeds, depths of cut, and cutting speeds, allowing for an evaluation of process performance under varied conditions. The findings from this study are expected to contribute both to academic understanding and practical process optimization. The comparative evaluation of cutting forces and surface roughness under the two turning strategies will show the conditions under which rotational turning can be a viable or even preferable alternative to longitudinal turning. In addition, the results of the role of tool inclination angle in rotational turning can inform tool design and process planning decisions, particularly in high-feed or energy-sensitive applications.

Although several recent studies have examined rotational turning individually, most of them focus either on force prediction or on surface quality alone [12,15,16,43,44], without integrating energy efficiency into the evaluation. Moreover, many of the available investigations are limited to narrow ranges of feeds or tool geometries, which does not reflect the higher feed rates increasingly demanded in modern production. Comparative studies for different turning procedures are particularly uncommon, and very few provide a simultaneous analysis of cutting forces, specific cutting forces, total work input, and detailed surface roughness metrics under identical conditions [45-47]. These gaps in the literature highlight the need for a comprehensive assess-

ment of how tool inclination and cutting parameters jointly influence both energy use and surface quality. The present study addresses these shortcomings by providing a complete experimental comparison and by quantifying the energy-to-surface-quality relationship.

Modern manufacturing increasingly requires machining processes that simultaneously improve energy efficiency and surface integrity while maintaining high productivity [48,49]. Traditional longitudinal turning often struggles to meet these requirements at elevated feeds due to increased cutting forces and weakened surface quality [50,51]. These limitations motivated the present research, which aims to clarify whether rotational turning (with its characteristic inclined cutting edge and altered tool-workpiece kinematics) can offer a more energy-efficient alternative with better surface quality. The central objective of this study is therefore to provide a systematic, experimentally verified comparison between rotational and longitudinal turning in terms of cutting forces, specific cutting forces, total mechanical work, and the resulting surface roughness. In conclusion, this study is a timely and necessary contribution to the evolving development on sustainable and high-performance machining. By evaluating rotational turning in direct comparison with traditional longitudinal turning, and by doing so through an energy- and surface-focused analysis, the work aligns with current industry priorities and scientific interests.

2. MATERIALS AND METHODS

An experimental procedure was employed for the comparative analysis of rotational and conventional turning processes. To evaluate the cutting forces in rotational turning, a previously developed force measurement system was utilized [5]. The current section details the experimental setup, including the machine tool, workpiece material, cutting tools, and applied cutting parameters. In addition, the methods used for cutting force measurement, energy calculation, and surface roughness evaluation are presented.

2.1 Experimental Setup

The experimental setup is shown in Figure 2. The cutting experiments were carried out on a Perfect-Jet MCV-M8 machining centre (with high-speed spindle and adequate rigidity to ensure consistent cutting conditions).

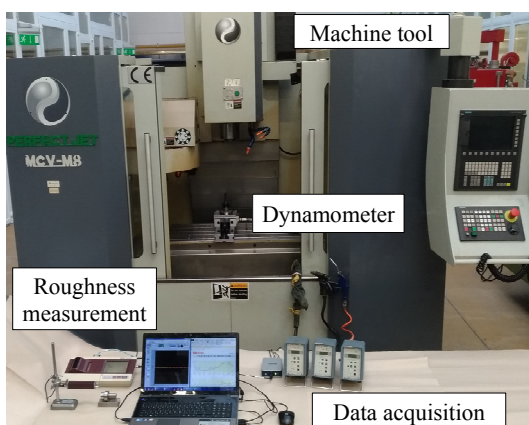


Figure 2. Experimental setup



Figure 3. Cutting tools used in the experiment

To reduce friction and heat generation during the machining process, a 5% emulsion of Rhenus TS 25 coolant and lubricant was applied through external spraying, providing both cooling and lubrication in the cutting zone. The workpieces were normalized C45 medium-carbon steel shafts, chosen for their industrial relevance and good machinability. Each specimen had a cylindrical surface to be machined with a diameter of 40 mm, a length of 12 mm, and a Vickers hardness of 220 HV. The normalization heat treatment ensured uniform microstructure and mechanical properties across the workpieces. Three different tool configurations were tested, including two rotational turning tools and one conventional longitudinal turning tool. These are illustrated in Figure 2:

- Tool A (Rotational, 30° inclination): Fraisa P5300682 end mill (HM MG10), with a 30° inclination angle and 20 mm diameter.
- Tool B (Rotational, 45° inclination): Sandvik Coromant 1P341-1600-XB end mill, where 3 of 4 cutting edges were ground down, ensuring only a single active cutting edge during operation. The inclination angle was 45°, with a diameter of 16 mm and tool material of grade 1630.
- Tool C (Conventional longitudinal turning tool): Sandvik Coromant insert CNMG 120412-PM, mounted in a DCLNL 2525 M 12 holder, with a tool grade of 4325.

The cutting tests were designed to provide variation in three primary cutting parameters to study the energy efficiency in a wide range of setups. Based on the machined material and the cutting tools, different values for the setup parameters were chosen for the experiments according to the recommendations of tool manufacturers, industrial practices and previous experiences: depth of cut (a_p): 0.1 mm, 0.2 mm, 0.3 mm; feed (f): 0.2 mm/rev, 0.6 mm/rev, 1.0 mm/rev; cutting speed (v_c): 200 m/min, 250 m/min. The selected combination of these resulted in a comprehensive matrix of setups, ensuring that the influence of each parameter and tool geometry could be evaluated. Table 1 summarizes all combinations of parameters used in the experimental program.

Each experimental setup is uniquely identified using a two-part designation: a letter indicating the tool used and a number corresponding to the cutting parameter combination. The setup number (1–12) refers to a specific combination of depth of cut, feed, and cutting speed, as summarized in Table 1. For example, Setup A3 refers to the experiment performed with Tool A under the cutting conditions defined as Setup 3 ($a_p = 0.1$ mm, $f = 1.0$ mm/rev, $v_c = 200$ m/min), while Setup C12 indicates an experiment performed with Tool C under the conditions of Setup 12 ($a_p = 0.3$ mm, $f = 1.0$ mm/rev,

$v_c = 200$ m/min). All tests were carried out using standardized clamping configurations optimized for each turning procedure, ensuring process stability and proper alignment. Although the fixturing systems for the rotational and longitudinal turning tools differed due to their geometric and functional requirements, each setup was designed to provide repeatable and rigid tool holding, minimizing external variability and ensuring the reliability of force and surface measurements.

Table 1. Experimental setup

Setup number	a_p [mm]	f [mm/rev]	v_c [m/min]
1	0.1	0.2	200
2	0.1	0.6	200
3	0.1	1	200
4	0.1	0.2	250
5	0.1	0.6	250
6	0.1	1	250
7	0.2	0.2	200
8	0.2	0.6	200
9	0.2	1	200
10	0.3	0.2	200
11	0.3	0.6	200
12	0.3	1	200

2.2 Measurement Methods

The cutting forces were recorded in real-time using a Kistler 9257A three-component piezoelectric dynamometer, which was mounted between the machine table and the tool fixture. The dynamometer measured the force components F_x , F_y and F_z in the machine coordinate system. These signals were transmitted through three Kistler 5011 single-channel charge amplifiers, converted to voltage signals, and digitized using a National Instruments NI-9215 Analog Input Module housed in a cDAQ-9171 chassis. Data acquisition was performed using NI LabVIEW software, with a sampling frequency of 1000 Hz, ensuring high temporal resolution of the cutting process. The raw force data were continuously recorded during each machining pass. Since the dynamometer measures forces in the machine coordinate system, a transformation was required to convert these into the tool coordinate system. Using the known and continuously changing relative position of the tool and the workpiece, the following force components were calculated for each time point in the function of the elapsed time (t):

- $F_c(t)$ – Main cutting force (tangential component)
- $F_f(t)$ – Feed force (axial component)
- $F_p(t)$ – Passive or thrust force (radial component)

Surface roughness characterization was conducted using the following procedure. Profile measurements were carried out with a Mitutoyo Surf Test SJ-301 portable surface roughness tester. Measurements were taken on three generatrix lines evenly spaced around the turned surface of each sample. The registered profiles were processed and analysed using Alti Map Premium 6.2.7487 software, in accordance with ISO 21920: 2021. The cut-off length was selected based on feed rate: 0.8 mm for 0.2 mm/rev feed rate; 2.5 mm for the 0.6 and 1.0

mm/rev feed rates. The focus of the roughness analysis was on R_a (arithmetical mean roughness) and R_z (maximum peak-to-valley height), calculated as the mean of the three 2D measurements per setup. These values were analysed as functions of feed rate and tool geometry, allowing for comparison between rotational and longitudinal turning processes. The measurement procedures ensured compliance with metrological standards, while the dual-device approach enabled a deeper understanding of the profile characteristics.

3. RESULTS

This section presents the measured and calculated results from the turning experiments conducted with the three different tool configurations (Tools A, B, and C) under twelve machining setups each. The complete dataset is summarized in Table 2, which includes all 36 unique setups (A1–A12, B1–B12, C1–C12) and the corresponding measured and calculated results.

The investigated output parameters include the maximum cutting forces in the tool coordinate system (tangential force F_c , feed force F_f , and passive force F_p), the corresponding specific cutting forces, the total mechanical work performed during cutting (W_i), and the surface roughness parameters: arithmetical mean roughness (R_a) and maximum peak-to-valley height (R_z).

The maximum values of the $F_c(t)$, $F_f(t)$, and $F_p(t)$ curves during the constant cross-section phase of cutting were determined for each setup and used as representative values. From these, the specific cutting forces in each direction (k_c , k_f , k_p) were calculated by dividing the measured cutting force by the cross-sectional area of the uncut chip:

$$k_i = \frac{F_i}{a_p \cdot f} \quad (i = c, f, p) \quad (1)$$

This allowed for comparison of tool loading under varying conditions, normalized by material removal volume.

The mechanical work done (W_i) during cutting was calculated by evaluating the contribution of force and motion in both the tangential (cutting) and axial (feed) directions. Since no primary movement occurs in the radial direction, the corresponding force component was neglected in the work calculation. Mathematically, the work in each direction was computed as:

$$W_i = \int_0^{t_0} F_i(t) \cdot v_i dt \quad (i = c, f) \quad (2)$$

where $F_i(t)$ is the time-dependent force component and v_i is the corresponding velocity component in direction i (either c = tangential or f = axial).

For each experimental setup, the total work was obtained as the sum of the work in the tangential and axial directions, calculated by integrating the product of the force and velocity components with respect to time during the constant cross-section phase of the cut. The total mechanical work was then:

$$W_t = W_c + W_f \quad (3)$$

Table 2. Experimental results of the maximum cutting force components, the corresponding specific cutting forces, the total mechanical work performed during cutting, and the surface roughness parameters

Setup	F_c	F_f	F_p	k_c	k_f	k_p	W_t	R_{a1}	R_{a2}	R_{a3}	R_a	R_{z1}	R_{z2}	R_{z3}	R_z
	[N]	[N]	[N]	$\left[\frac{\text{N}}{\text{mm}^2} \right]$	$\left[\frac{\text{N}}{\text{mm}^2} \right]$	$\left[\frac{\text{N}}{\text{mm}^2} \right]$	[J]	[μm]							
A01	79.6	20.2	48.3	3979	1012	2413	621	0.47	0.48	0.49	0.48	3.82	3.79	3.73	3.78
A02	178.3	51.2	90.6	2972	854	1510	468	0.73	0.69	0.74	0.72	5.18	5.19	5.67	5.35
A03	268.9	80.4	126.9	2689	804	1269	419	1.15	1.08	1.14	1.12	7.39	6.57	7.35	7.10
A04	77.7	20.6	46.8	3885	1032	2339	605	0.45	0.45	0.44	0.45	3.81	3.80	3.78	3.80
A05	176.1	52.1	89.3	2935	869	1488	462	0.76	0.74	0.78	0.76	5.95	5.19	5.39	5.51
A06	265.0	81.6	120.1	2650	816	1201	420	1.63	1.62	1.57	1.61	9.44	8.94	9.90	9.43
A07	149.1	41.3	79.8	3728	1032	1995	1162	0.53	0.53	0.53	0.53	4.42	4.36	4.30	4.36
A08	333.9	102.7	155.0	2783	856	1292	870	0.81	0.75	0.78	0.78	5.78	5.62	5.59	5.66
A09	501.4	159.3	235.3	2507	797	1176	795	1.93	1.81	1.91	1.88	10.03	9.30	9.20	9.51
A10	222.7	65.3	103.7	3712	1089	1729	1724	0.47	0.51	0.49	0.49	3.76	3.67	3.55	3.66
A11	548.3	174.2	248.1	3046	968	1378	1400	0.85	0.81	0.92	0.86	5.24	5.28	5.89	5.47
A12	840.0	279.1	341.0	2800	930	1137	1287	1.98	2.17	1.76	1.97	9.42	9.46	8.55	9.14
B01	81.1	28.7	38.0	4057	1434	1898	624	0.78	0.71	0.71	0.73	5.24	5.23	4.73	5.07
B02	186.2	72.6	69.2	3103	1211	1153	466	2.03	1.97	1.92	1.97	10.93	10.35	10.19	10.49
B03	273.5	111.1	88.2	2735	1111	882	412	4.96	4.93	4.97	4.95	22.44	22.43	22.20	22.36
B04	81.7	30.2	39.4	4087	1511	1970	622	0.46	0.78	0.69	0.64	5.47	5.28	5.06	5.27
B05	181.4	74.8	66.2	3023	1247	1104	458	2.25	2.12	2.08	2.15	11.31	10.70	10.16	10.72
B06	265.4	113.7	79.3	2654	1137	793	403	5.13	4.85	5.08	5.02	23.71	21.97	21.91	22.53
B07	163.1	63.7	74.1	4076	1593	1853	1206	0.74	0.74	0.71	0.73	5.24	5.15	5.05	5.15
B08	362.2	160.9	112.1	3019	1341	934	876	2.02	2.05	1.92	2.00	11.21	10.03	9.62	10.29
B09	528.3	247.3	125.2	2641	1237	626	774	5.48	5.70	5.51	5.56	23.95	23.14	22.46	23.18
B10	246.1	106.1	98.7	4102	1768	1645	1804	0.68	0.72	0.72	0.71	4.90	4.83	4.51	4.75
B11	536.4	263.1	125.6	2980	1462	698	1309	2.14	2.04	2.04	2.07	11.07	10.88	9.52	10.49
B12	804.8	407.1	146.1	2683	1357	487	1173	4.36	4.75	4.13	4.41	21.15	20.77	18.97	20.30
C01	80.8	16.9	89.3	4038	847	4463	647	0.96	0.99	0.94	0.96	4.44	5.00	4.46	4.63
C02	176.4	20.5	161.6	2940	342	2694	466	6.68	6.49	6.57	6.58	25.74	25.54	25.67	25.65
C03	272.8	23.9	239.9	2728	239	2399	432	12.83	13.51	13.09	13.14	50.70	50.86	50.63	50.73
C04	78.7	18.0	94.4	3933	900	4722	630	0.99	0.92	1.02	0.98	4.77	4.42	4.84	4.68
C05	174.4	19.9	164.6	2906	332	2743	466	6.69	6.65	6.86	6.73	26.08	26.16	26.55	26.26
C06	286.6	28.6	253.0	2866	286	2530	453	13.29	13.56	13.35	13.40	51.81	52.27	51.47	51.85
C07	137.2	38.4	144.2	3429	961	3604	1099	0.92	0.91	0.93	0.92	4.58	4.44	4.50	4.51
C08	302.7	46.9	232.2	2523	391	1935	815	7.14	7.13	7.12	7.13	27.21	27.38	27.24	27.28
C09	459.3	52.5	319.3	2297	262	1596	727	13.88	14.12	13.44	13.81	53.14	52.53	51.67	52.45
C10	188.6	61.1	171.4	3143	1019	2857	1513	0.94	0.91	0.92	0.92	4.56	4.40	4.59	4.52
C11	425.7	79.4	287.7	2365	441	1598	1133	7.02	6.90	6.94	6.95	26.83	26.93	26.77	26.84
C12	649.1	82.4	395.8	2164	275	1319	1043	13.57	13.79	13.52	13.63	54.22	52.68	52.50	53.13

4. DISCUSSION

This section provides a detailed analysis of the experimental results obtained from the comparative study of rotational and longitudinal turning. The discussion focuses on five main aspects: the evolution of the cutting force components, the behaviour of specific cutting forces, the total mechanical work input during machining, the resulting surface roughness characteristics, and the relation between the finished surface roughness and the work done. Each of these parameters is evaluated as a function of the setup parameters and compared across the three tool types.

4.1 Cutting Force Components

The cutting forces acting during turning provide essential understanding into the mechanical load acting on the

tool and workpiece. In this study, the tangential (F_c), feed (F_f), and passive (F_p) force components were measured for all three tool types (A, B, C) under twelve identical machining parameter sets. Figure 4–6 show the alteration of the maximum values of the three main force components.

An increase in the depth of cut from 0.1 mm to 0.3 mm generally resulted in substantial growth in all force components for all tool types. For example, in rotational turning with Tool A at constant feed ($f = 0.2 \text{ mm/rev}$, $v_c = 200 \text{ m/min}$), F_c rose from 79.6 N (Setup A01) to 222.7 N (A10) – an increase of approximately 179.8%. Similarly, F_f grew from 20.2 N to 65.3 N (+223.2%), and F_p from 48.3 N to 103.7 N (+114.7%). This trend is consistent for Tools B and C as well. With Tool C, under the same cutting conditions (Setups C01, C07, C10), F_c increased from 80.8 N to 188.6 N (+133.4%), showing that longitudinal turning also exhibits strong

dependence on a_p , although Tool A generated lower forces for the same a_p increment. This suggests more efficient chip engagement and reduced load per unit depth in rotational turning – likely due to the inclined cutting edge modifying the effective rake and chip thickness.

The feed rate significantly influenced all three force components. With Tool A, increasing feed from 0.2 to 1.0 mm/rev (Setups A01 to A03, $a_p = 0.1$ mm, $v_c = 200$ m/min) caused F_c to grow from 79.6 N to 268.9 N, marking a 237.7% increase. F_f grew even more sharply: from 20.2 N to 80.4 N (+298.0%), indicating a strong correlation between feed and axial loading. F_p rose from 48.3 N to 126.9 N (+162.7%). Similar behaviour is observed for Tools B and C. For example, Tool C at $a_p = 0.1$ mm, $v_c = 200$ m/min (Setups C01 → C03) showed F_c increasing from 80.8 N to 272.8 N (+237.5%), and F_p from 89.3 N to 239.9 N (+168.6%). The steeper rise in F_f with Tool B (from 28.7 N to 111.1 N, +287.4%) displays the additional axial engagement due to the inclined cutting edge, especially at higher feeds. In general, higher feeds increase uncut chip thickness, which proportionally affects both F_c and F_f . However, the rate of increase is also influenced by tool geometry. The rotational tools (A and B) show slightly more moderate force growth than Tool C, especially in the feed direction, suggesting that rotational turning may reduce axial tool loading at high feeds – a potential advantage in high-feed machining.

The influence of cutting speed (from 200 m/min to 250 m/min) on cutting forces was more moderate than that of a_p and f . For example, Tool A at $f = 0.2$ mm/rev and $a_p = 0.1$ mm showed a slight decrease in F_c from 79.6 N to 77.7 N (-2.4%) and in F_p from 48.3 N to 46.8 N (-3.1%). This mild reduction is potentially attributed to thermal softening of the workpiece material at higher speeds and possibly improved chip flow. However, the effect is not universally consistent across all conditions. With Tool B, at $f = 0.2$ mm/rev and $a_p = 0.1$ mm (B01 → B04), F_c remained nearly unchanged (81.1 N to 81.7 N), while F_f increased from 28.7 N to 30.2 N (+5.2%). With Tool C, F_c decreased slightly (C01 → C04: 80.8 N → 78.7 N, -2.6%) and F_p increased (89.3 N → 94.4 N, +5.7%). This variation indicates that while speed can influence force levels, it interacts more subtly with cutting edge engagement and tool wear than feed or depth of cut. When comparing tool types directly under identical conditions, significant differences appear. For example, at Setup 03, F_c values were Tool A: 268.9 N, Tool B: 273.5 N, Tool C: 272.8 N. These results indicate similar tangential force levels across all tools at high feed and low depth, suggesting that chip load per edge dominates in this range. In contrast, the feed force varied more significantly: Tool A: 80.4 N, Tool B: 111.1 N, Tool C: 23.9 N. Tool C showed much lower axial force, which is expected, as axial force in longitudinal turning acts parallel to the feed, while in rotational turning (especially with inclined tools), axial load includes components redirected by the tool inclination. However, the F_f of Tool B was 38.1% higher than of Tool A, showing that the 45° inclination induces greater axial load than the 30° tool at high feed. The radial force also showed tool-dependent differences. For

instance, at Setup 09, F_p values were Tool A: 235.3 N, Tool B: 125.2 N, Tool C: 319.3 N.

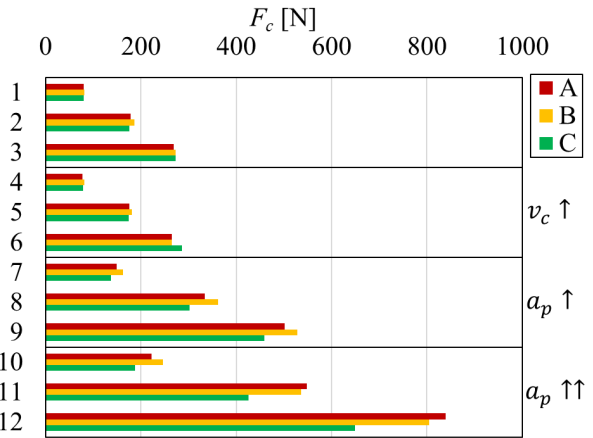


Figure 4. Maximum tangential cutting force (F_c) for all setups using Tools A, B, and C

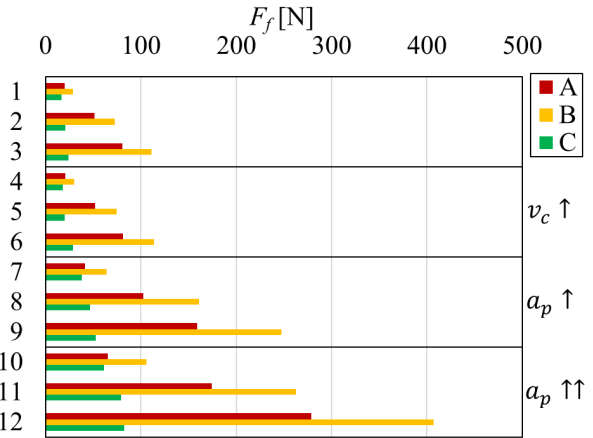


Figure 5. Maximum feed directional force (F_f) recorded in the experiments for each tool and setup combination

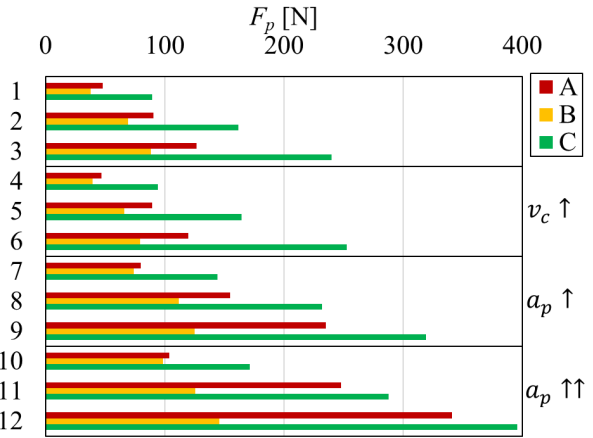


Figure 6. Maximum passive force (F_p) measured during the cutting tests across all tool configurations and parameters

Here, Tool C produced the highest radial force, while Tool B yielded the lowest. This may be attributed to the inclined cutting action in Tools A and B, which distributes force more toward the feed and tangential directions and reduces direct thrust into the workpiece.

Overall, the comparison of the cutting force components suggests that rotational turning tools – especially the 30° version, Tool A – can reduce radial and axial loads, especially at high feeds and low-to-medium dep-

ths. While tangential force trends are similar across all tools, the distribution of force components differs significantly, and this can influence tool deflection, part accuracy, and surface integrity in downstream analysis.

4.2 Specific Cutting Forces

The specific main cutting force, specific feed force, and specific passive force offer normalized measures of cutting load by expressing the force required per unit of uncut chip cross-section. Figures 7–9 present the specific values of the cutting force components, calculated as shown in Equation 1.

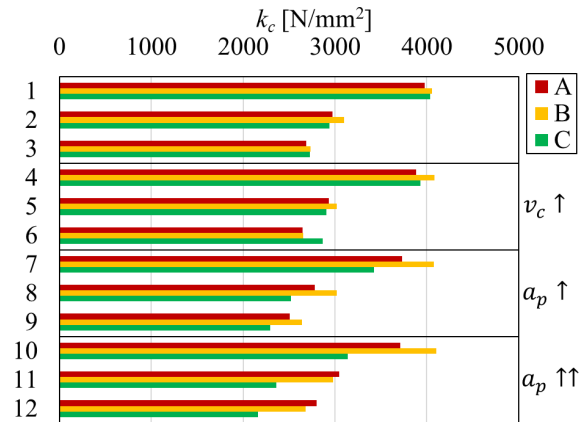


Figure 7. Specific cutting force in the tangential direction (k_c) calculated for each experimental setup

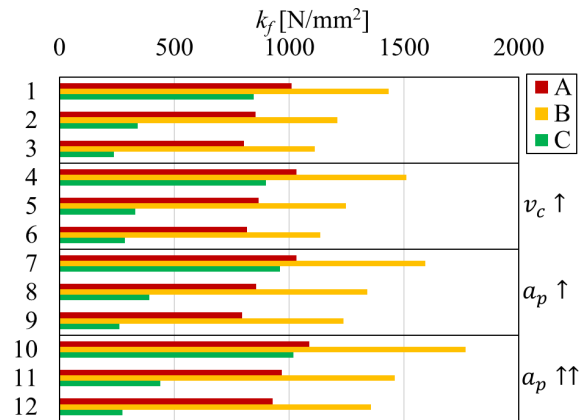


Figure 8. Specific feed directional cutting force (k_f) determined for the three tool types and cutting conditions

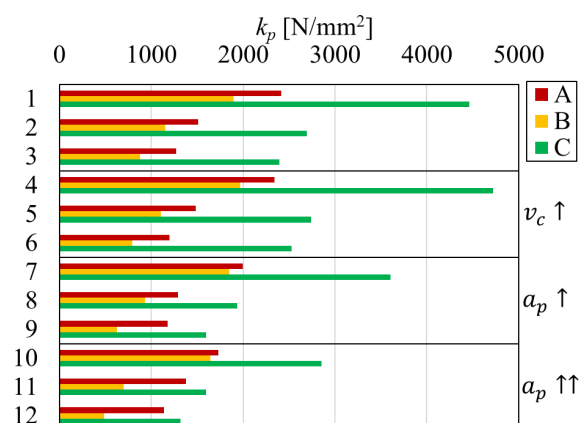


Figure 9. Specific passive cutting force (k_p) obtained for all machining setups.

These parameters enable better comparison across different feed rates and depths of cut, eliminating size effects. This section discusses how these specific force values are influenced by the cutting parameters and tool geometry and highlights the differences between rotational turning tools (A and B) and the conventional longitudinal turning tool (C).

Feed rate had a strong influence on the specific cutting forces, particularly k_c . With increasing feed, k_c showed a clear decreasing trend, which is consistent with classical machining theory: as uncut chip thickness increases, the force per unit area tends to decrease due to improved shearing efficiency and the reduced influence of the edge radius. For instance, with Tool A at $a_p = 0.1$ mm and $v_c = 200$ m/min (Setups A01 to A03), k_c decreased from 3979.3 N/mm² ($f = 0.2$ mm/rev) to 2689.2 N/mm² ($f = 1.0$ mm/rev), a 32.4% reduction; k_f dropped from 1011.7 to 803.7 N/mm² (−20.6%); k_p declined from 2413.1 to 1269.3 N/mm² (−47.4%). Similar reductions were observed with Tool B: k_c dropped from 4057.3 to 2735.2 N/mm² (−32.6%), k_f fell from 1434.4 to 1111.3 N/mm² (−22.5%); k_p decreased from 1898.5 to 882.1 N/mm² (−53.5%). Tool C followed the same pattern but started from slightly higher k_c at low feed and declined to even lower levels at high feed (k_c fell from 4038.1 to 2728.3 N/mm², −32.5%). This inverse relationship highlights the economic potential of increasing feed rate, especially when tool deflection and surface integrity errors are acceptable. Interestingly, k_p dropped much more sharply with increasing feed than k_c , indicating that radial force is more sensitive to chip thickness. This could be due to better chip curling and evacuation at higher feeds, reducing resistance perpendicular to the cutting direction.

Contrary to the feed rate, increasing depth of cut generally resulted in stable or slightly increasing specific cutting forces, depending on the tool. For example, with Tool A at constant feed ($f = 0.2$ mm), k_c changed only slightly: A01 ($a_p = 0.1$): 3979.3 N/mm², A07 ($a_p = 0.2$ mm): 3728.4 N/mm² (−6.3%), A10 ($a_p = 0.3$ mm): 3711.9 N/mm² (−0.4%). This indicates that k_c becomes more consistent at higher a_p , showing that cutting is more volume-dominant and less affected by edge effects. Tool B and Tool C showed similar trends. In Tool C at $f = 0.2$ mm/rev, k_c decreased from 4038.1 N/mm² ($a_p = 0.1$ mm) to 3143.0 N/mm² ($a_p = 0.3$ mm), a 22.2% decrease. Interestingly, despite Tool C being a traditional longitudinal tool, it showed a more pronounced reduction in k_c with increasing a_p . This may be due to less effective chip engagement at lower a_p in longitudinal turning, where tool nose radius and clearance become more critical.

The cutting speed (from 200 to 250 m/min) had a relatively minor effect on k_c , k_f , and k_p across all tool types. For example, with Tool A at $a_p = 0.1$ mm, $f = 0.2$ mm k_c decreased slightly from 3979.3 (A01) to 3884.8 N/mm² (A04), a −2.4% reduction. Similar small reductions were observed in Tool B (−1.7%) and Tool C (−2.6%). These reductions are likely due to thermal softening of the workpiece material and reduced friction at higher cutting speeds. However, the influence remains moderate in the investigated range. Comparing

specific forces under identical conditions reveals important tool-dependent differences. For example, at Setup 03 ($a_p = 0.1$ mm, $f = 1.0$ mm/rev, $v_c = 200$ m/min), k_c values were: Tool A: 2689.2 N/mm², Tool B: 2735.2 N/mm², Tool C: 2728.3 N/mm². The k_c values are nearly identical here, suggesting that at high feed and low depth, all three tools engage similar chip section areas. However, the differences in k_f are more revealing: Tool A: 803.7 N/mm², Tool B: 1111.3 N/mm², Tool C: 238.6 N/mm². The significantly lower k_f of Tool C (by about 70%) at the same setup indicates that axial loading is substantially reduced in longitudinal turning, as expected. Conversely, rotational tools induce more axial stress due to the inclination of the cutting edge. Radial specific forces also varied considerably: Tool A: 1269.3 N/mm², Tool B: 882.1 N/mm², Tool C: 2398.7 N/mm². Here, Tool C exhibited the highest radial specific load, over 89% higher than Tool A, and nearly 172% higher than Tool B. This suggests that rotational turning reduces radial force per unit area – a major advantage in minimizing tool deflection and improving dimensional accuracy. Looking at larger cuts (Setup 12: $a_p = 0.3$ mm, $f = 1.0$ mm, $v_c = 200$ m/min), the k_c values were 2799.9 N/mm² in A12, 2682.6 N/mm² in B12, and 2163.6 N/mm² in C12. Here, Tool C shows the lowest k_c , likely due to improved material shearing at greater chip loads. However, its k_p remains the highest (1319.3 N/mm² compared to 1136.8 N/mm² for A12 and 487.0 N/mm² for B12), confirming that radial loading remains a concern in longitudinal turning.

The analysis of the specific forces revealed interesting alterations. Increasing feed consistently reduces k_c , k_f , and k_p across all tools. Increasing a_p results in more stable k_c values, with minor reductions or plateaus. Cutting speed causes slight reductions in specific forces, attributed to thermal effects. Rotational tools reduce k_p , especially Tool B, which shows the lowest radial specific load. Longitudinal turning (Tool C) shows lowest axial specific forces but highest radial ones, indicating a trade-off between stability and part deflection. These findings confirm that rotational turning – especially with higher inclination – can redistribute the cutting load, potentially lowering radial deflection values and enabling higher feeds while maintaining manageable tool stresses.

4.3 Total Work Done

The total mechanical work done during the cutting process is a fundamental metric of energy demand in machining. In our study, it reflects the combined force and displacement contributions in the tangential and feed directions over the duration of material removal. In this study, the total work was determined by integrating the product of force and velocity over time in the cutting and feed directions, neglecting the radial direction due to the lack of relative motion in that axis. This section explores the effects of cutting parameters and tool geometry on the energy requirement per cut and compares the three tool types to assess the implications for energy-efficient machining. Figure 10 shows the results of the calculations based on Equations 2–3.

The feed rate had a definite and consistent effect on W_t across all tools and depths of cut. For instance, at $a_p = 0.1$ mm and $v_c = 200$ m/min, Tool A showed the following W_t values: 620.8 Jin A01, 468.2 J in A02, 419.4 J in A03. Although the material removal rate increased significantly, the total work decreased with higher feed. Between A01 and A03, W_t dropped by 32.5%, even though the feed was multiplied by a factor of five. This counterintuitive result highlights the efficiency gains of high-feed machining: although direct cutting forces increase, the shorter cutting time and lower specific forces result in reduced total energy input. Similar trends were observed with Tools B and C. For example, with Tool C under the same conditions the following results were calculated: 646.5 J in C01, 466.3 J in C02 (−27.9%), 431.9 J in C03 (−33.2%). This consistent decrease in W_t with increasing feed further supports the recommendation for using higher feeds – within surface quality and machine rigidity constraints – as a strategy for reducing energy consumption.

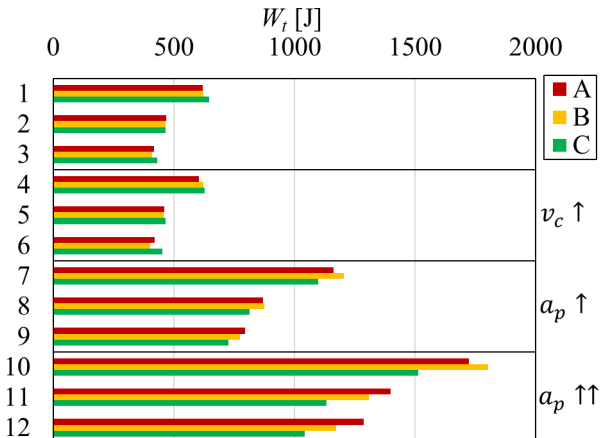


Figure 10. Total mechanical work done (W_t) during the cutting process for each setup and tool configuration.

Contrary to the feed effect, increasing the depth of cut significantly increased the total work done, due to the larger volume of material removed and higher resistance encountered. For instance, with Tool A at $f = 0.2$ mm and $v_c = 200$ m/min the following work values were calculated: 620.8 Jin A01, 1162.3 Jin A07, 1723.7 Jin A10. From A01 to A10, W_t increased by 177.6%, closely proportional to the growth in cross-sectional area of the cut. Similar proportional increases were observed with the other tools. For example, the following were determined for Tool C: 646.5 Jin C01, 1099.4 J in C07 (+70.1%), 1512.8 J in C10 (+134%). Although Tool C also showed rising work with a_p , the relative increase was less steep than for Tool A, likely due to higher k_c of Tool C at low a_p , which becomes less dominant as a_p increases and cutting stabilizes.

The cutting speed had a minimal impact on total work done. For instance, with Tool A at $a_p = 0.1$ mm and $f = 0.2$ mm/rev W_t was 620.8 Jin A01 and 605.0 J in A04 (−2.5%). This minor reduction may be attributed to decreased cutting forces at higher speed due to thermal softening. However, the effect is generally negligible compared to feed and depth of cut. Similar small reductions were seen across Tools B and C (for example, C01 → C04 shows a −2.6% difference in the results).

At identical cutting conditions, significant differences in W_t were observed among the three tools. For Setup 03, the total work was: 419.4 Jin A03, 411.6 Jin B03, 431.9 Jin C03. Here, Tools A and B (rotational) required slightly less work (-2.9% and -4.7%) than Tool C. This confirms that, despite higher direct force magnitudes, the overall energy requirement is slightly reduced in rotational turning under high-feed, low-ap conditions. More pronounced differences emerged at deeper cuts. At Setup 12, the following work values were calculated: 1286.6 Jin A12, 1173.4 Jin B12, 1043.5 Jin C12. Tool C showed the lowest W_t , likely due to more favourable chip flow and material shearing at high volumes in longitudinal turning. However, this comes at the cost of higher radial and axial loading, as shown in earlier sections. Interestingly, Tool B consistently showed the lowest energy requirement in many conditions despite its 45° inclination, which tends to increase axial loading. This suggests that its geometry may offer a favourable rake angle and chip flow that minimizes resistance during chip formation. Across all 36 setups, the mean total work values were: 926.2 J for Tool A, 889.2 J for Tool B, and 902.6 J for Tool C. While these values are relatively close, Tool B shows a slight overall advantage (~4% lower W_t). This difference, though moderate, may translate into significant savings in large-scale or continuous machining environments, supporting the industrial relevance of rotational turning.

The calculation of the work done led to the following observations. Increasing feed noticeably reduces W_t , due to shortened engagement time and decreased k_c . Increasing depth of cut leads to proportional increases in energy input. Cutting speed has a minor effect on total work. Rotational tools (A and B) require less energy than longitudinal Tool C at high feed-low ap conditions. Tool B (45°) showed the lowest average energy requirement, suggesting that its edge inclination may be optimal for chip engagement and cutting efficiency. These findings confirm that rotational turning is not only viable but can be more energy efficient than conventional turning under appropriate cutting conditions, especially when configured with well-designed tool geometries.

4.4 Surface Roughness

Surface roughness is a key indicator of the quality and functional performance of a machined part, influencing wear, friction and fatigue behaviour. In this study, both R_a (arithmetical mean roughness) and R_z (peak-to-valley height) were measured to characterize the surface topography of the turned parts. Their average values are presented in Figure 11 (R_a) and in Figure 12 (R_z).

Feed rate showed the strongest influence on surface roughness. Across all tools, increasing the feed from 0.2 mm/rev to 1.0 mm/rev led to significant increases in both R_a and R_z . This trend aligns with theoretical expectations: higher feed rates increase the spacing and depth of tool marks on the surface, resulting in rougher textures. For example, using Tool A at $a_p = 0.1$ mm and $v_c = 200$ m/min resulted in the following: R_a increased from 0.48 μm (A01) to 1.123 μm (A03), which is a +134% increase; R_z rose from 3.78 μm to 7.103 μm , a

+87.9% increase. Tool B showed even more intense changes: R_a went from 0.733 μm (B01) to 4.953 μm (B03) (+575%), while R_z rose from 5.066 μm to 22.356 μm (+341%). Tool C (longitudinal) also exhibited steep increases: R_a : 0.963 μm → 13.143 μm (+1265%), R_z : 4.633 μm → 50.73 μm (+995%). These results clearly demonstrate that longitudinal turning is much more sensitive to feed increase in terms of surface roughness. The use of a single-point insert in Tool C produces a regular feed mark profile, which becomes deeper and wider at higher feed rates. In contrast, rotational tools A and B, which cut with an inclined edge and produce overlapping tool paths, generate more compressed surface features even at high feed.

Depth of cut had a much weaker influence on surface roughness compared to feed. For Tool A at $f = 0.2$ mm and $v_c = 200$ m/min, R_a remained stable: 0.48 μm (A01), 0.53 μm (A07), 0.49 μm (A10). Furthermore, R_z values were: 3.78 μm → 4.36 μm → 3.66 μm (minor variation). Similarly, Tool B and C showed only minor differences across a_p levels at constant feed (for Tool C: R_a : 0.963 μm (C01) → 0.92 μm (C07) → 0.923 μm (C10); R_z : 4.633 μm → 4.506 μm → 4.516 μm). These results indicate that a_p does not significantly alter the roughness profile, as the surface finish is dominated by the kinematics of feed marks and not by the depth of material removed. This behaviour confirms that the surface roughness is mostly generated by the feed motion and cutting edge geometry rather than the chip cross-section.

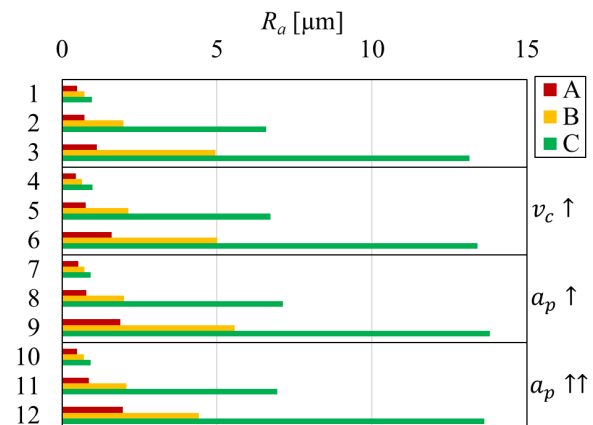


Figure 11. Arithmetic mean surface roughness (R_a) values of the machined surfaces

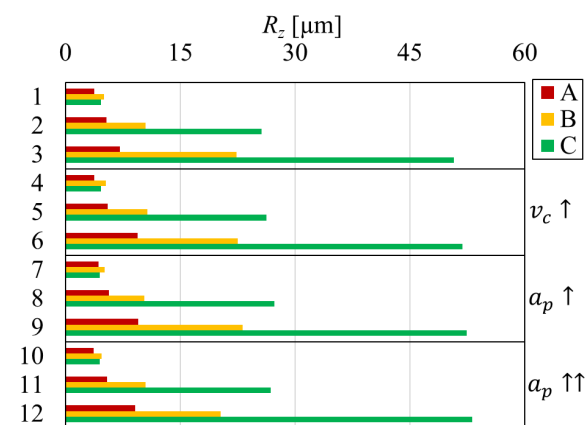


Figure 12. Maximum peak-to-valley height (R_z) surface roughness values for each tool and cutting condition

Increasing the cutting speed had a slightly beneficial effect on surface roughness. For example, with Tool A at $a_p = 0.1$ mm and $f = 0.2$ mm, R_a dropped from 0.48 μm (A01) to 0.446 μm (A04) (-7.1%), R_z changed from 3.78 μm to 3.796 μm , essentially unaffected. Tool C showed a similar trend: R_a : 0.963 μm (C01) \rightarrow 0.976 μm (C04) ($+1.4\%$); R_z : 4.633 μm \rightarrow 4.676 μm ($+0.9\%$). Overall, changing the cutting speed from 200 m/min to 250 m/min does not significantly affect surface roughness. Slight improvements are likely due to better chip softening and reduced built-up edge formation at higher speeds. However, this influence is minor compared to the overwhelming effect of feed rate.

The performance of the three tools with respect to surface roughness was notably different, especially at high feed values. At Setup 03, the following values were measured: R_a : Tool A: 1.123 μm , Tool B: 4.953 μm , Tool C: 13.143 μm ; R_z : Tool A: 7.103 μm , Tool B: 22.356 μm , Tool C: 50.73 μm . Tool A, the 30° rotational tool, delivered the best surface finish at high feed. Tool B (45°) produced significantly rougher surfaces, likely due to the more aggressive inclination and a less favourable chip exit path. Tool C performed the worst in terms of roughness at high feed, producing R_a values more than 11 times higher than Tool A in some setups. Even at moderate feed values ($f = 0.6$ mm/rev), this trend persists. At $a_p = 0.2$ mm the R_a values were: Tool A: 0.78 μm , Tool B: 1.996 μm , Tool C: 7.13 μm ; and the R_z values were: Tool A: 5.663 μm , Tool B: 10.286 μm , Tool C: 27.276 μm . This confirms that rotational turning offers superior surface quality at raised feeds. The inclined cutting edge and tool motion of the rotational tools result in overlapping paths that reduce peak heights and flatten valleys, leading to smoother surfaces. Additionally, the variation between the three R_a and R_z measurements per setup was low (standard deviation $<10\%$ in most cases), indicating good repeatability in all cases.

The analysis of the surface roughness across the different setups revealed the following results. Feed rate has the greatest impact on R_a and R_z , with higher feed drastically increasing roughness. Depth of cut and cutting speed have minimal effects on surface finish in this range. Rotational turning, especially with Tool A, enables lower roughness values, even at high feed. Tool B produces moderate roughness, while Tool C results in significantly rougher surfaces, particularly as feed increases. The surface roughness results validate the application of rotational turning tools in high-feed operations where surface quality is still required. These tools make it possible to combine high productivity with acceptable or superior surface finish, offering a substantial advantage in industrial applications.

4.5 Energy Efficiency in Relation to Achieved Surface Roughness

In addition to analysing cutting forces and roughness independently, a more integrated view of energy efficiency can be obtained by examining how much energy is required to produce a surface with a given quality. By comparing the total mechanical work done (W_t) during cutting to the resulting surface roughness

values (R_a and R_z), valuable insights can be drawn about the process efficiency of each tool type. Although longitudinal turning with Tool C frequently resulted in the highest W_t values, it also produced the roughest surfaces, especially at higher feeds. For example, in Setup C03, where the feed was 1.0 mm/rev and the cutting speed 200 m/min, the resulting R_a was 13.14 μm and R_z reached 50.73 μm , while the work done was 431.9 J. While this setup seems efficient in terms of energy per micrometre of roughness, the actual surface finish is far beyond acceptable in most technical applications. In contrast, Tool A, representing the 30° rotational turning variant, achieved significantly better surface finishes with only somewhat lower energy input. At Setup A03, with the same feed and cutting speed, the surface roughness was reduced to 1.12 μm R_a and 7.10 μm R_z , with a comparable work input of 419.4 J. This means that roughly the same energy was used to produce a surface that was over ten times smoother in terms of R_a . Tool B, with a 45° inclination, produced intermediate results both in terms of energy and surface finish. In Setup B03, the work done was slightly lower than Tool A (411.6 J), but the surface roughness was significantly worse at 4.95 μm R_a . These results suggest that from an energy-per-quality perspective, Tool A delivers the most favourable balance when moderate or good surface finish is required, while Tool C, despite sometimes appearing efficient in a mathematical sense, does not provide surfaces of sufficient quality. Therefore, rotational turning – especially with a lower inclination angle – allows not only for higher productivity but also better energy efficiency in achieving technical surface requirements, making it an advantageous choice for applications that demand both performance and sustainability.

5. CONCLUSION

This study presents a comparative investigation of rotational and longitudinal turning processes, focusing on energy efficiency and surface roughness during the machining of normalized medium-carbon steel shafts. Machining energy and surface quality are critical parameters in modern manufacturing, as they directly impact both process sustainability and the functional performance of components. The primary goal of this research was to evaluate how the use of rotational turning tools with different inclination angles (30° and 45°) influences cutting forces, specific cutting forces, total work input and resulting surface roughness, compared to conventional longitudinal turning. The experimental methodology involved machining 40 mm diameter, 12 mm long normalized C45 steel workpieces under controlled cutting conditions. Depth of cut, feed per revolution, and cutting speed were systematically varied, producing twelve experimental setups for each tool. Cutting forces in tangential, axial, and radial directions were recorded using a three-component dynamometer, and the total work done, as well as specific cutting forces, were calculated from these measurements. Surface roughness was evaluated both in terms of arithmetic mean roughness and peak-to-valley height, using a combination of 2D and 3D surface measurement techniques.

The results demonstrate clear trends in the relationship between tool geometry, cutting conditions, energy consumption and surface finish. Rotational turning with a 30° inclination achieved the best balance between low energy consumption and acceptable surface quality, particularly at moderate-to-high feeds. Rotational turning at 45° increased productivity but at the cost of higher R_a values for the same energy input. Longitudinal turning consistently produced rougher surfaces, and although the energy per unit roughness sometimes appeared lower, the absolute surface quality was insufficient for most technical applications. Analysis of specific cutting forces confirmed that rotational turning reduces cutting load in all directions compared to conventional longitudinal turning, contributing to improved energy efficiency.

The three main findings that highlight the novelty of this work are:

- Rotational turning can significantly reduce specific cutting forces while maintaining or improving surface quality.
- The energy required to produce a given surface roughness is lower with rotational turning than with longitudinal turning.
- The tool inclination angle has a measurable impact on the energy–surface quality interaction, which can guide process optimization.

The findings of this study are relevant to a wide range of engineering applications in which cylindrical steel components are produced in high volume, such as in automotive shafts, power-transmission elements, and general-purpose machine components. In such production environments, even marginal improvements in energy consumption or achievable surface quality translate into significant economic and environmental benefits. Rotational turning is emerging as a promising process variant, but its practical capabilities and limitations remain insufficiently characterized. By providing experimentally validated data on energy demand and surface finish across realistic industrial cutting parameters, this work delivers engineering-useful guidance for selecting tool geometry, inclination angle, and cutting conditions. The results enable practitioners to reduce machining energy, increase productive feed rates, and achieve target roughness levels more reliably. Thus, the study contributes both scientifically—by clarifying process mechanics—and practically—by supporting informed decision-making in process planning.

Future research could extend these findings by exploring additional inclination angles, investigating other workpiece materials or hardened steels, analysing microstructural effects of rotational turning, and integrating the results into predictive models for energy-efficient process planning. Furthermore, the combined influence of lubrication conditions and tool wear could be assessed to develop guidelines for sustainable high-performance turning operations.

ACKNOWLEDGMENT

The creation of this scientific communication was supported by the University of Miskolc with funding

granted to the author IstvánSztankovics within the framework of the institution's Scientific Excellence Support Program. (Project identifier: ME-TKTP-2025-089)

REFERENCES

- [1] Abdelaoui, F.Z.E., Jabri, A., Barkany, A.E.: Optimization techniques for energy efficiency in machining processes—a review, *The International Journal of Advanced Manufacturing Technology* Vol. 125, pp. 2967–3001,2023. <https://doi.org/10.1007/s00170-023-10927-y>
- [2] Neugebauer, R., Drossel, W., Wertheim, R., Hochmuth, C., Dix, M.: Resource and energy efficiency in machining using High-Performance and Hybrid processes, *Procedia CIRP* Vol. 1, pp. 3–16,2012. <https://doi.org/10.1016/j.procir.2012.04.002>
- [3] Bartarya, G., Choudhury, S.K.: State of the art in hard turning, *International Journal of Machine Tools and Manufacture*, Vol. 53, pp. 1–14,2011. <https://doi.org/10.1016/j.ijmachtools.2011.08.019>
- [4] Sousa, V.F.C., Silva, F.J.G.: Recent Advances in Turning Processes Using Coated Tools—A Comprehensive Review, *Metals*, Vol. 10, 170,2020. <https://doi.org/10.3390/met10020170>
- [5] Sharma, V.S., Dogra, M., Suri, N.M.: Advances in the turning process for productivity improvement — a review, *Proceedings of the Institution of Mechanical Engineers Part B Journal of Engineering Manufacture*, Vol. 222, pp. 1417–1442, 2008. <https://doi.org/10.1243/09544054jem1199>
- [6] Sharma, V., Pandey, P.M.: Recent advances in turning with textured cutting tools: A review, *Journal of Cleaner Production*, Vol. 137, pp. 701–715,2016. <https://doi.org/10.1016/j.jclepro.2016.07.138>
- [7] Tschätsch, H.: *Applied Machining Technology*, Springer Berlin, Heidelberg 2009. <https://doi.org/10.1007/978-3-642-01007-1>
- [8] Hosokawa, A., Ueda, T., Onishi, R., Tanaka, R., Furumoto, T.: Turning of difficult-to-machine materials with actively driven rotary tool, *CIRP Annals*, Vol. 59, pp. 89–92. 2010. <https://doi.org/10.1016/j.cirp.2010.03.053>
- [9] Sofuoğlu, M.A., Çakır, F.H., Kuşhan, M.C., Orak, S.: Optimization of different non-traditional turning processes using soft computing methods, *Soft Computing*, Vol. 23, pp. 5213–5231,2018. <https://doi.org/10.1007/s00500-018-3471-8>
- [10] Klocke, F., Bergs, T., Degen, F., Ganser, P.: Presentation of a novel cutting technology for precision machining of hardened, rotationally symmetric parts, *Production Engineering*, Vol. 7, pp. 177–184. 2012. <https://doi.org/10.1007/s11740-012-0438-y>
- [11] Kundrák, J., Gyáni, K., Deszpóth, I. Sztankovics, I.: Some Topics in Process Planning of Rotational Turning, *Engineering Review*, Vol. 34, pp. 23–32,2014. Available online: <https://engineeringreview.org/index.php/ER/article/view/349>(accessed on 25August 2025).

[12] Martíkáň, P., Czán, A., Holubják, J., Varga, D., Martinček, J. and Czánová, T.: Verification of New Method of Determining the Roughness Parameters for Rotational Turning with Non-linear Cutting Edge, *Procedia Engineering*, Vol. 192, pp. 563–568, 2017. <https://doi.org/10.1016/j.proeng.2017.06.097>

[13] Kummer, N.: *Method and device for machining rotationally symmetrical surfaces of a workpiece*. Patent number: DE102004026675C5, 2004.

[14] J. G. Weisser Söhne GmbH & Co. KG: Rotational Turning. Available online: <https://www.weisser-web.com/en/rotational-turning> [Accessed 2508 2023].

[15] Degen, F., Klocke, F., Bergs, T., Ganser, P.: Comparison of rotational turning and hard turning regarding surface generation, *Production Engineering*, Vol. 8, pp. 309–317, 2014. <https://doi.org/10.1007/s11740-014-0530-6>

[16] Sztankovics, I., Kundrák, J.: Effect of the inclination angle on the defining parameters of chip removal in rotational turning, *Manufacturing Technology*, Vol. 14, pp. 97–104, 2014. <https://doi.org/10.21062/ujep/x.2014/a/1213-2489/mt/14/197>

[17] May, G., Barletta, I., Stahl, B., Taisch, M.: Energy management in production: A novel method to develop key performance indicators for improving energy efficiency, *Applied Energy*, Vol. 149, pp. 46–61, 2015. <https://doi.org/10.1016/j.apenergy.2015.03.065>

[18] Axinte, D.A., Gindy, N., Fox, K., Unanue, I.: Process monitoring to assist the workpiece surface quality in machining, *International Journal of Machine Tools and Manufacture*, Vol. 44, pp. 1091–1108, 2004. <https://doi.org/10.1016/j.ijmachtools.2004.02.020>

[19] Sugimoto, K.-I.: Recent progress of Low and Medium-Carbon advanced martensitic steels, *Metals*, Vol. 11, 652, 2021. <https://doi.org/10.3390/met11040652>

[20] Das, I., Zaman, P.B.: Response Modeling and Optimization of Process Parameters in Turning Medium Carbon Steel Under Minimum Quantity Lubrication (MQL) with Vegetable Oil and Oil Blends, *Lubricants*, Vol. 12, 444. 2024. <https://doi.org/10.3390/lubricants12120444>

[21] Duplak, J., Duplakova, D., Zajac, J.: Research on roughness and microhardness of C45 material using High-Speed Machining, *Applied Sciences*, Vol. 13, 7851, 2023. <https://doi.org/10.3390/app13137851>

[22] Shunmugesh, K., Kurian, S., Khan, M.A., Kumar, D.S., Mishra, P.: Maximizing efficiency in C45 steel machining: an integrated AI-based approach to coated insert optimization, *International Journal on Interactive Design and Manufacturing*, Vol. 19, pp. 831–848, 2024. <https://doi.org/10.1007/s12008-024-02124-2>

[23] Pálmai, Z., Kundrák, J., Felhő, C., Makkai, T.: Investigation of the transient change of the cutting force during the milling of C45 and X5CrNi18-10 steel taking into account the dynamics of the electro-mechanical measuring system, *The International Journal of Advanced Manufacturing Technology*, Vol. 133, pp. 163–182, 2024. <https://doi.org/10.1007/s00170-024-13640-6>

[24] Nur, R., Yusof, N.M., Sudin, I., Nor, F.M., Kurniawan, D.: Determination of Energy Consumption during Turning of Hardened Stainless Steel Using Resultant Cutting Force, *Metals*, Vol. 11, 565, 2021. <https://doi.org/10.3390/met11040565>

[25] Ma, J., Ge, X., Chang, S.I., Lei, S.: Assessment of cutting energy consumption and energy efficiency in machining of 4140 steel, *The International Journal of Advanced Manufacturing Technology*, Vol. 74, pp. 1701–1708, 2014. <https://doi.org/10.1007/s00170-014-6101-3>

[26] Nguyen, T.-T.: An energy-efficient optimization of the hard turning using rotary tool, *Neural Computing and Applications*, Vol. 33, pp. 2621–2644, 2020. <https://doi.org/10.1007/s00521-020-05149-2>

[27] Kundrák, J., Karpuschewski, B., Pálmai, Z., Felhő, C., Makkai, T., Borysenko, D.: The energetic characteristics of milling with changing cross-section in the definition of specific cutting force by FEM method, *CIRP Journal of Manufacturing Science and Technology*, Vol. 32, pp. 61–69, 2020. <https://doi.org/10.1016/j.cirpj.2020.11.006>

[28] Petre, I.M., Găvrus, C.: Influence of the cutting force upon machining process efficiency, *Materials Today Proceedings*, Vol. 72, pp. 586–593, 2022. <https://doi.org/10.1016/j.matpr.2022.10.063>

[29] Abainia, S., Ouelaa, N.: Predicting the dynamic behaviour of the turning tool vibrations using an experimental measurement, numerical simulation and analytical modelling for comparative study, *The International Journal of Advanced Manufacturing Technology*, Vol. 115, No. 7–8, pp. 2533–2552, 2021. <https://doi.org/10.1007/s00170-021-07275-0>

[30] Sadredine, A., Nouredine, O., Cherif, D.: Modeling and experimental validation of dynamic response of the cutting tool in turning operations. *FME Transaction*, Vol. 48, No. 2, pp. 454–459, 2020. <https://doi.org/10.5937/fme2002454s>

[31] Qin, Z., Jiang, S., Yin, S., Sun, Y., Wang, M.: Chatter stability prediction methods in the machining processes: a review. *The International Journal of Advanced Manufacturing Technology*, Vol. 136, No. 7–8, pp. 2945–2985, 2025. <https://doi.org/10.1007/s00170-024-14971-0>

[32] Yuvaraju, B., Nanda, B., Srinivas, J.: Investigation of stability in internal turning using a boring bar with a passive constrained layer damping. *FME Transaction*, Vol. 49, No. 2, pp. 384–394, 2021. <https://doi.org/10.5937/fme2102384y>

[33] Zhang, B., Deng, W., Zhong, P.: Theoretical model and experimental investigation of machined surface roughness considering plastic side flow. *CIRP Journal of Manufacturing Science and Technology*, Vol. 61, pp. 353–367, 2025. <https://doi.org/10.1016/j.cirpj.2025.06.020>

[34] Machno, M., Zębala, W., Franczyk, E.: Optimization of turning of Inconel 625 to improve surface quality after finishing process, *Materials*, Vol. 17, No. 23, 6009, 2024. <https://doi.org/10.3390/ma17236009>

[35] Kowalczyk, M.: Analysis of cutting forces and geometric surface structures in the milling of NITI alloy. *Materials*, Vol. 17, No. 2, 488, 2024. <https://doi.org/10.3390/ma17020488>

[36] Korkut, I., Donertas, M.: The influence of feed rate and cutting speed on the cutting forces, surface roughness and tool–chip contact length during face milling, *Materials & Design*, Vol. 28, No. 1, pp. 308–312, 2005. <https://doi.org/10.1016/j.matdes.2005.06.002>

[37] Motorcu, A., Ekici, E.: Evaluation and multi-criteria optimization of surface roughness, deviation from dimensional accuracy and roundness error in drilling CFRP/Ti6Al4 stacks, *FME Transaction*, Vol. 50, No. 3, pp. 441–460, 2022. <https://doi.org/10.5937/fme2203441m>

[38] Bai, L., Yang, Q., Cheng, X., Ding, Y., Xu, J.: A hybrid physics-data-driven surface roughness prediction model for ultra-precision machining, *Science China Technological Sciences*, Vol. 66, No. 5, pp. 1289–1303, 2023. <https://doi.org/10.1007/s11431-022-2358-4>

[39] Patel, D., Thakker, H., Kiran, M., Vakharia, V.: Surface roughness prediction of machined components using gray level co-occurrence matrix and Bagging Tree, *FME Transaction*, Vol. 48, No. 2, pp. 468–475, 2020. <https://doi.org/10.5937/fme2002468p>

[40] Lalwani, D., Mehta, N., Jain, P.: Experimental investigations of cutting parameters influence on cutting forces and surface roughness in finish hard turning of MDN250 steel, *Journal of Materials Processing Technology*, Vol. 206, No. 1–3, pp. 167–179, 2008. <https://doi.org/10.1016/j.jmatprotec.2007.12.018>

[41] Deepanraj, B., Raman, L., Senthilkumar, N. and Shivasankar, J.: Investigation and optimization of machining parameters influence on surface roughness in turning AISI 4340 steel, *FME Transaction*, Vol. 48, No. 2, pp. 383–390, 2020. <https://doi.org/10.5937/fme2002383b>

[42] Kowalczyk, M.: Application of Taguchi method to optimization of surface roughness during precise turning of NiTi shape memory alloy, in: *Proceedings of SPIE, the International Society for Optical Engineering*, Vol. 10445, 104455G, 2017. <https://doi.org/10.1117/12.2281062>

[43] Martíkáň, P., Holubják, J., Czanova, T., Pustay, J., Joch, R.: Identification of roughness parameter when turning process with helical cutting edge for machining of automotive transmission parts, *Transportation Research Procedia*, Vol. 40, pp. 362–366, 2019. <https://doi.org/10.1016/j.trpro.2019.07.053>

[44] Joch, R., Pilc, J., Daniš, I., Drbúl, M., Krajčoviech, S.: Analysis of surface roughness in turning process using rotating tool with chip breaker for specific shapes of automotive transmission shafts, *Transportation Research Procedia*, Vol. 40, pp. 295–301, 2019. <https://doi.org/10.1016/j.trpro.2019.07.044>

[45] Kumar, R., Bilga, P. S., Singh, S.: Multi objective optimization using different methods of assigning weights to energy consumption responses, surface roughness and material removal rate during rough turning operation, *Journal of Cleaner Production*, Vol. 164, pp. 45–57, 2017. <https://doi.org/10.1016/j.jclepro.2017.06.077>

[46] Grzesik, W., Wanat, T.: Comparative assessment of surface roughness produced by hard machining with mixed ceramic tools including 2D and 3D analysis, *Journal of Materials Processing Technology*, Vol. 169, No. 3, pp. 364–371, 2005. <https://doi.org/10.1016/j.jmatprotec.2005.04.080>

[47] Lin, W., Lee, B., Wu, C.: Modeling the surface roughness and cutting force for turning, *Journal of Materials Processing Technology*, Vol. 108, No. 3, pp. 286–293, 2001. [https://doi.org/10.1016/s0924-0136\(00\)00835-9](https://doi.org/10.1016/s0924-0136(00)00835-9)

[48] Pawanr, S., Gupta, K.: A review on recent advances in the energy efficiency of machining processes for sustainability, *Energies*, Vol. 17, No. 15, 3659, 2024. <https://doi.org/10.3390/en17153659>

[49] Goindi, G. S., Sarkar, P.: Dry machining: A step towards sustainable machining – Challenges and future directions, *Journal of Cleaner Production*, Vol. 165, pp. 1557–1571, 2017. <https://doi.org/10.1016/j.jclepro.2017.07.235>

[50] Sousa, V. F. C., Silva, F. J. G.: Recent Advances in Turning Processes Using Coated Tools—A Comprehensive Review, *Metals*, Vol. 10, No. 2, 170, 2020. <https://doi.org/10.3390/met10020170>

[51] Pawanr, S., Gupta, K.: Dry Machining Techniques for Sustainability in Metal Cutting: A review, *Processes*, Vol. 12, No. 2, 417, 2024. <https://doi.org/10.3390/pr12020417>

[52] Chen, Z., Peng, R. L., Zhou, J., M'Saoubi, R., Gustafsson, D., Moverare, J.: Effect of machining parameters on cutting force and surface integrity when high-speed turning AD 730 with PCBN tools, *The International Journal of Advanced Manufacturing Technology*, Vol. 100 No. 9–12, 2601–2615, 2018. <https://doi.org/10.1007/s00170-018-2792-1>

[53] Sztankovics, I.: Design and realization of a cutting force measuring system to analyze the chip removal process in rotational turning, *Metrology*, Vol. 5, No. 1, 5, 2025. <https://doi.org/10.3390/metrology5010005>

КОМПАРАТИВНА СТУДИЈА РОТАЦИОНОГ И УЗДУЖНОГ СТРУГАЊА: ЕНЕРГЕТСКА ЕФИКАСНОСТ И ХРАПАВОСТ ПОВРШИНЕ ПРИ ОБРАДИ НОРМАЛИЗОВАНОГ СРЕДЊЕУГЉЕНИЧНОГ ЧЕЛИКА

И. Станковић, Д. Родић

Ова студија упоређује ротационо и уздушно стругање током обраде нормализованог средњеугљеничног челика. Циљ је да се процене разлике у енергетској ефикасности и квалитету површине. Тестирана су три алата: два ротациона стругарска алата са угловима нагиба од 30° и 45° и конвенционални уздушни стругарски алат. Извршено је тридесет шест експеримената резања уз различите дубине резања, помака и брзине резања. Силе резања су мерење у три правца и коришћене за израчунавање специфичних сила резања и укупног механичког рада. Храпавост површине је процењена

коришћењем параметара аритметичке средње храпавости и максималне висине од врха до дна. Резултати показују да ротационо стругање, посебно са нагибом од 30° , смањује специфичне силе резања и омогућава мању потрошњу енергије уз упоредиву продуктивност. Такође пружа бољу завршну обраду површине при средњим и високим помацима. Уздушно стругање је генерисало прихватљиве нивое енергије, али је произвело знатно храпавије површине. Резултати истичу улогу нагиба алата у побољшању интеракција између енергије и квалитета површине.